https://doi.org/10.5194/egusphere-2025-491
Preprint. Discussion started: 21 February 2025

SIMPLE EULERIAN-LAGRANGIAN APPROACH TO SOLVE EQUATIONS FOR SINKING PARTICULATE ORGANIC MATTER IN THE OCEAN

Vladimir Maderich[1], Igor Brovchenko[1], Kateryna Kovalets[1], Seongbong Seo[2], and Kyeong Ok Kim[2]

[1]Institute of Mathematical Machine and System Problems, Glushkov av., 42, Kyiv 03187, Ukraine
[2]Korea Institute of Ocean Science and Technology, Busan, Republic of Korea

Correspondence: Kyeong Ok Kim (kokim@kiost.ac.kr)

Abstract. A gravitational sinking of the particulate organic matter (POM) is a key mechanism of vertical transport of carbon in the deep ocean and its subsequent sequestration. The size spectrum of these particles is formed in the euphotic layer by the primary production and various mechanisms including food web consumption. The mass of particles, as they descend, changed under aggregation, fragmentation, bacterial decomposition which depends on the water temperature and oxygen concentration, particle sinking velocity, age of the organic particles, ballasting and other factors. In this paper, we developed simple Eulerian-Lagrangian approach to solve equations for sinking particulate matter when the influence of the size and age of particles, temperature and oxygen concentration on their dynamics and degradation processes were taken into account. The model considers feedback between degradation rate and particle sinking velocity. We rely on the known parameterizations, but our Eulerian-Lagrangian approach to solving the problem differs, allowing the algorithm to be incorporated into biogeochemical global ocean models with relative ease. Two novel analytical solutions of a system of the one-dimensional Eulerian equation for POM concentration and Lagrangian equations for particle mass and position were obtained for constant and age-dependent degradation rates. At a constant rate of particle sinking, they correspond to exponential and power-law profiles of the POM concentration. It was found that feedback between degradation rate and sinking velocity results to a significant change in POM and POM flux vertical profiles. The calculations are compared with the available measurement data for POM and POM flux for the latitude band of 20-30°N in the Atlantic and Pacific Oceans and 50-60°S in the Southern Ocean. The dependence of the degradation rate on temperature significantly affected the profiles of POM concentration enhancing the degradation of sinking particles in the ocean's upper layer and suppressing it in the deep layer of the ocean. The influence of oxygen concentration in all cases considered was insignificant compared to the distribution of temperature with depth.

https://doi.org/10.5194/egusphere-2025-491
Preprint. Discussion started: 21 February 2025

1 Introduction

A gravitational sinking of the particulate organic matter (POM) is a key mechanism of vertical transport of carbon in the deep ocean (gravitational biological pump) and its subsequent sequestration (Siegel et al., 2023). The biological pump mechanism provides not only the transfer and burial of carbon, but also nutrients, trace metals, natural and artificial radionuclides through the scavenging mechanism (Roca-Martí and Puigcorbé, 2024; Maderich et al., 2022). The size spectrum of sinking particles is formed in the euphotic layer by the primary production and various mechanisms, including aggregation and fragmentation under the influence of mechanical factors (Burd, 2024) and through food web consumption. The mass of particles, as they descend in deep layers of the ocean, decreases under the influence of grazing by filter feeders and bacterial decomposition which depends on the water temperature and oxygen concentration (Cram et al., 2018), particle falling velocity (Alcolombri et al., 2021), age of the organic particle (Jokulsdottir and Archer, 2016; Aumont et al., 2017) and other factors such as ballasting (Armstrong et al., 2002). The POM degradation rate can be proportional to the particle volume (DeVries et al., 2014; Cram et al., 2018) or the surface area (Omand et al., 2020; Alcolombri et al., 2021).

Many biogeochemical models assume that the settling velocity of particles is constant with depth. Then, depending on the degradation rate, the POM vertical profile can be found. At a constant degradation rate, the corresponding vertical profile of particle mass concentration and mass flux will be exponential (Banse, 1990; Lutz et al., 2002). Assuming that the degradation rate is inversely proportional to the age of particle (Middelburg, 1989), the vertical profile of particle mass concentration and mass flux can be found as a power law (Cael et al., 2021). This power law corresponds to the well-known empirical "Martin curve" (Martin et al., 1987). However, as the particle mass decreases due to remineralization, the rate at which the particle falls also decreases. This feedback, along with other factors except for the age of the particle, is taken into account in several mechanistic models (e.g., DeVries et al., 2014; Cram et al., 2018; Omand et al., 2020; Alcolombri et al., 2021). An analytical solution to the equation for the distribution of POM by particle size was obtained by DeVries et al. (2014) for a constant degradation rate. However, as noted by DeVries et al. (2014), the values of the vertical flux of POM mass at great depths turned out to be 1-2 orders of magnitude less than observed. It can be assumed that this discrepancy is due to the constancy of the degradation rate with depth in the model. A decrease in the rate of degradation can be caused by a decrease in water temperature (Cram et al., 2018) and an increase in the age of sinking particles with depth.

In this paper, we developed simple Eulerian-Lagrangian approach to solve equations for sinking particulate matter when the influence of the size and age of particles, temperature and oxygen concentration on their dynamics and degradation processes were taken into account. We rely on the known parameterizations (Kriest and Oshlies, 2008; DeVries et al., 2014; Cram et al., 2018; Omand et al., 2020), but our Eulerian - Lagrangian approach to solving the problem is different, allowing the model to be incorporated into biogeochemical global ocean models with relative ease. The paper is organized as follows: the equations of the model for sinking particulate organic matter are given in Section 2. The analytical solutions for constant and age-dependent degradation rates were obtained and compared with available data on vertical concentration and mass flux of the POM in Section 3. The numerical Eulerian-Lagrangian method for the generalized model is given in Section 4. The results of the

https://doi.org/10.5194/egusphere-2025-491
Preprint. Discussion started: 21 February 2025

simulations are discussed in Section 5. Our findings are summarized in Section 6. The equivalence of the obtained solution and the solution (DeVries et al., 2014) for a constant rate of degradation is shown in Appendix A.

2 Model equations

We consider the vertical flux of the organic particles caused by gravitational forces. The vertical distribution of these particles below the euphotic layer z_{eu} is governed by the flux of settling particles equilibrated by particle degradation due to bacterial decomposition. The processes of aggregation and fragmentation are not included in the model. It is assumed steady state of the particle flux. The Eulerian particle concentration transport equation and the Lagrangian equations for the individual particles are solved. The Eulerian equation for the POM concentration $C_{p,d}$ [kg m^{-3}] with particle diameter d [m] is written as

$$\frac{\partial W_{p,d} C_{p,d}}{\partial z'} + \gamma C_{p,d} = 0, \tag{1}$$

where $W_{p,d}$ [m d^{-1}] is the settling velocity of a particle of diameter d; z' [m] is the vertical coordinate directed downward from the depth of euphotic zone ($z' = z - z_{eu}$); γ [d^{-1}] is the degradation rate. The boundary condition for (1) is

$$z' = 0: \quad C_{p,d} = C_{p,d}(0), \tag{2}$$

where $C_{p,d}(0)$ is a prescribed POM concentration on the lower boundary of the euphotic layer z_{eu}.

The Stokes-type settling velocity $W_{p,d}$ depends on the density difference between the density of water and the density of particles, the particle shape, and kinematic viscosity. To take into account the whole ensemble of aforementioned factors that impact the sinking we approximated the sinking law by power dependence which is widely used in the particle flux models (e.g. (DeVries et al., 2014)):

$$W_{p,d} = \frac{\partial z'}{\partial t} = c_w d^{\eta}, \tag{3}$$

where t is time, η ($\eta \leq 2$) is the dimensionless scaling argument and c_w [m$^{1-\eta}$ d^{-1}] is a prefactor coefficient. Note that Figure 1 from (Cael et al., 2021) demonstrates the difficulties of describing the sinking speed of particles of various sizes, shapes and structures with a single universal dependence. Therefore, relation (3) should be considered only as a first approximation in describing the complex dynamics of particles.

Consider the particle dynamics in the Lagrangian coordinate system. The mass of the particle m_d is related to the particle diameter d as

$$m_d = c_m d^{\zeta}, \tag{4}$$

where ζ ($\zeta \leq 3$) is the dimensionless scaling argument and c_m is a prefactor coefficient (DeVries et al., 2014). Equation (4) takes into account the fact that with an increase in particle size, the porosity of organic particles increases (Mullin, 1966).

We restrict consideration to the case when the mass of a particle descending with velocity $W_{p,d}$ decreases over time t as a result of microbial degradation. This process can be described by a first-order reaction with a reaction rate γ [d^{-1}]. The

https://doi.org/10.5194/egusphere-2025-491
Preprint. Discussion started: 21 February 2025

corresponding equation for m_d is written as

$$\frac{\partial m_d}{\partial t} = -\gamma(\theta) m_d^{\theta}. \tag{5}$$

Parameter $\theta = 1$ when the degradation rate is proportional to the particle volume and $\theta = 2/3$ when the degradation rate is proportional to the surface area of the particle (Omand et al., 2020).

In general case, the degradation rate depends on many factors. Here we take into account only several of them: the age of the organic particle t, the temperature of sea water T, and the concentration of oxygen $[O_2]$

$$\gamma = \gamma(t, T(z'), [O_2](z')). \tag{6}$$

Details of the parameterization (6) will be given in Section 4.

3 Analytical solutions

3.1 Age-independent degradation rate

First, we consider the case when the degradation rate of the particle is age-independent (Age-Independent Degradation rate (AID) model). Furthermore, suppose that the mass loss is proportional to the particle volume ($\gamma = \gamma_0$, $\theta = 1$) and it does not depend on temperature and oxygen concentration ($\gamma_0 = \text{const}$). Then solution of Eq. (5) is

$$m_d = m_{0d} \exp(-\gamma_0 t), \tag{7}$$

where $m_{0d} = c_m d_0^{\zeta}$ is the initial value of particle mass of diameter d_0. Initially, these particles are placed at depth $z = z'$. The diameter of the particle varies with time as

$$d = d_0 \exp\left(-\frac{\gamma_0 t}{\zeta}\right). \tag{8}$$

Assuming the quasi-equilibrium descending of the particle in the Stokes regime we estimated the dependence of $W_{p,d}$ on t using Eq. (8)

$$W_{p,d} = \frac{\partial z'}{\partial t} = c_w d_0^{\eta} \exp\left(-\frac{\eta\gamma_0 t}{\zeta}\right). \tag{9}$$

The vertical path z' travelled by a particle is

$$z' = \frac{\zeta c_w d_0^{\eta}}{\eta\gamma_0}\left[1 - \exp\left(-\frac{\eta\gamma_0 t}{\zeta}\right)\right]. \tag{10}$$

Eliminating time from Eqs. (9) and (8) by using (10) we obtained $W_{p,d}$ and d as the functions of z'

$$W_{p,d} = H(z') c_w d_0^{\eta} (1 - \psi z'), \tag{11}$$

$$d = H(z') d_0 (1 - \psi z')^{\frac{1}{\eta}}, \tag{12}$$

https://doi.org/10.5194/egusphere-2025-491
Preprint. Discussion started: 21 February 2025

where

$$\psi = \frac{\eta\gamma_0}{\zeta c_w d_0^{\eta}}. \tag{13}$$

The Heaviside function is $H(z') = 1$ if $z' \le \psi^{-1}$, and $H(z') = 0$ if $z' > \psi^{-1}$. Taking into account Eq. (11) we solved Eq. (1) to obtain

$$C_{p,d} = H(z')C_{p,d}(0)\,(1-\psi z)^{\frac{\zeta-\eta}{\eta}}. \tag{14}$$

The solution (14) describes the vertical profile of the POM concentration caused by the prescribed particle size distribution at $z' = 0$. This distribution can be approximated by power dependence $\sim d_0^{-\epsilon}$ (e.g., Kostadinov et al., 2009) where ϵ is a power-law exponent. To obtain the size distribution of $C_{p,d}(0)$ we use a small increment of particle size Δd_0 assuming that concentration is uniform within the interval Δd_0. Then distribution $C_{p,d}(0)$ is given by

$$C_{p,d}(0) = M_0 d_0^{-\epsilon} m_{0,d} \Delta d_0 = M_0 c_m d_0^{\zeta-\epsilon} \Delta d_0, \tag{15}$$

where M_0 is a constant which can be estimated from the total concentration of sinking POM at $z' = 0$. The total concentration C_p is calculated as sum of $C_{p,d}$ over n_d intervals

$$C_p(z') = \sum_{i=0}^{n_d} C_{p,d,i} = M_0 c_m \sum_{i=0}^{n} d_{0,i}^{\zeta-\epsilon} H(z')\,(1-\psi z')^{\frac{\zeta-\eta}{\eta}}\,\Delta d_0. \tag{16}$$

At $\Delta d_0 \to 0$ the total concentration of sinking POM C_p [kg m^{-3}] in the range from d_0^{min} to d_0^{max} can be calculated as

$$C_p(z') = M_0 c_m \int_{d_0^{min}}^{d_0^{max}} \tilde{d}_0^{\zeta-\epsilon} H(z')\,(1-\psi z')^{\frac{\zeta-\eta}{\eta}}\, d\tilde{d}_0. \tag{17}$$

Total mass flux F_p [kg m^{-2}d^{-1}] can be calculated in a similar way

$$F_p(z) = \sum_{i=0}^{n_d} C_{p,d,i} W_{p,d,i} = M_0 c_m c_w \sum_{i=0}^{n} (d_{0,i}^{\eta+\zeta-\epsilon} H(z')\,(1-\psi z')^{\frac{\zeta}{\eta}}\,\Delta d_0 \tag{18}$$

At $\Delta d_0 \to 0$:

$$F_p(z) = M_0 c_m c_w \int_{d_0^{min}}^{d_0^{max}} \tilde{d}_0^{\eta+\zeta-\epsilon} H(z')\,(1-\psi z')^{\frac{\zeta}{\eta}}\, d\tilde{d}_0. \tag{19}$$

The problem for which we obtained the solution (14) for POM concentration $C_{p,d}$ is similar to that solved by DeVries et al. (2014) for the particle size spectrum equation. In Appendix A we show the equivalence of these solutions.

3.2 Age-dependent degradation rate

The degradation rate as a function of POM age t [d] can be described following Middelburg (1989) as

$$\gamma(t) = \frac{\beta}{\alpha + t}, \tag{20}$$

https://doi.org/10.5194/egusphere-2025-491
Preprint. Discussion started: 21 February 2025

where α and β are empirical constants. We define such a model as an age-dependent degradation rate (ADD) model. The time dependencies for d and $W_{p,d}$ with parameterization of the degradation rate (20) are obtained similarly to Section 3.1. They are written as

$$d = d_0 \left(\frac{\alpha}{\alpha + t}\right)^{\beta/\zeta}, \tag{21}$$

$$W_{p,d} = c_w d^{\eta} \left(\frac{\alpha}{\alpha + t}\right)^{\eta\beta/\zeta}. \tag{22}$$

The path travelled by a sinking particle is

$$z' = c_w d_0^{\eta} \frac{\alpha\zeta}{\zeta - \eta\beta} \left[\left(1 + \frac{t}{\alpha}\right)^{(\zeta-\eta\beta)/\zeta} - 1\right]. \tag{23}$$

Eliminating time from Eqns. (20), (21) and (22) we obtained depth dependent solutions:

$$W_{p,d}(z') = c_w d_0^{\eta} \left(1 + \phi z'\right)^{-\frac{\eta\beta}{\zeta-\eta\beta}}, \tag{24}$$

$$\gamma(z') = \frac{\beta}{\alpha} \left(1 + \phi z'\right)^{-\frac{\zeta}{\zeta-\eta\beta}}, \tag{25}$$

$$d(z') = d_0 \left(1 + \phi z'\right)^{-\frac{\beta}{\zeta-\eta\beta}}, \tag{26}$$

where

$$\phi = \frac{\zeta - \eta\beta}{\alpha\zeta c_w d_0^{\eta}}. \tag{27}$$

Integrating Eqn. (1) with a boundary condition (2) and taking into account (24) and (25) we found a solution for $C_{p,d}$ as

$$C_{p,d}(z') = C_{p,d_0} \left(1 + \phi z'\right)^{\frac{(\eta-\zeta)\beta}{\zeta-\eta\beta}}. \tag{28}$$

Assuming that the density of distribution of particle mass concentration at $z = 0$ is approximated by power law (15) we can obtain the total concentration of sinking POM C_p in the range of d_0 from d_0^{min} to d_0^{max} as

$$C_p(z') = M_0 c_m \int_{d_0^{min}}^{d_0^{max}} \tilde{d}_0^{\zeta-\epsilon} \left(1 + \phi z'\right)^{\frac{(\eta-\zeta)\beta}{\zeta-\eta\beta}} d\tilde{d}_0. \tag{29}$$

The corresponding total mass flux $F_p(z)$ is written as

$$F_p(z') = \int_{d_0^{min}}^{d_0^{max}} W_{p,d} C_{p,d} d\tilde{d}_0 = M_0 c_m c_w \int_{d_0^{min}}^{d_0^{max}} \tilde{d}_0^{\eta+\zeta-\epsilon} \left(1 + \phi z'\right)^{-\frac{\zeta b}{\zeta-\eta\beta}} d\tilde{d}_0. \tag{30}$$

3.3 Comparison of analytical solutions

The obtained analytical solutions have several important properties. At a constant sinking velocity $W_{p,d} = W_p(d_0)$, the solution of (1) for constant degradation rate corresponds to the exponential profile of the particle concentration

$$C_p(z', d_0) = C_p(0, d_0) \exp\left(-\frac{\gamma_0 z'}{c_w d_0^{\eta}}\right), \tag{31}$$

https://doi.org/10.5194/egusphere-2025-491
Preprint. Discussion started: 21 February 2025

Table 1. The baseline model parameters.

Parameters	Value/range	Unit	Reference
η	1.17	-	Smayda (1970)
ζ	2.28	-	Mullin (1966)
γ_0	0.03	d^{-1}	Kriest and Oshlies (2008)
c_w	$2.2 \cdot 10^5$	$\mathrm{m}^{1-\eta}\mathrm{d}^{-1}$	Kriest and Oshlies (2008)
ϵ	4.2	-	Kostadinov et al. (2009)
Q_{10}	$2-3$	-	Cram et al. (2018)
T_{ref}	4	°C	Cram et al. (2018)
K_O	8	μ M	Cram et al. (2018)
α	30	d	Aumont et al. (2017)
β	1	-	Aumont et al. (2017)
d_0^{max}	2000	μm	DeVries et al. (2014)
d_0^{min}	20	μm	DeVries et al. (2014)
n_d	990	–	DeVries et al. (2014)

while for time-dependent degradation rate (20) it corresponds to the power-law distribution of the POM concentration

$$C_p(z', d_0) = C_p(0, d_0) \left(\frac{\alpha c_w d_0^\eta}{\alpha c_w d_0^\eta + z'} \right)^\beta. \tag{32}$$

Both these solutions are frequently used to approximate observed particle flux profiles, e.g. (Martin et al., 1987) and (Lutz et al., 2002). The corresponding profiles normalized to values at the base of the euphotic layer $C_p(z_{eu})$ and $F(z_{eu})$ are shown in Fig. 1 where C_p and F_p profiles were obtained by summation of n profiles in (16) and (18). The values of $C_p(z_{eu})$ and $F(z_{eu})$ were calculated using 15. The model parameters (η, ζ, γ_0, c_w, ϵ, α, β, d_0^{max}, d_0^{min},n) in Table 1 were as chosen by DeVries et al. (2014) and Aumont et al. (2017). As seen in Fig. 1, with such parameters C_p and F_p decay much faster for AID than for ADD model. Note that C_p and F_p tend to exponential or power-law profiles only at great depths. At the same time, at a constant particle velocity, the weighted vertical velocity of particles (Fig. 1c) for both AID and ADD models the speed increases with depth.

The presence of feedback between γ and $W_{p,d}$ leads to a significant change in these profiles. In the case of constant γ_0, the vertical distribution of concentration $C_{p,d}$ for one surface fraction of POM size d_0 is limited by a finite layer of thickness $h_0 = (\zeta c_w d_0^\eta)(\eta\gamma_0)^{-1}$. Particles in this layer sink at a linearly decreasing velocity. The mass of particles also decreases with depth to a depth where they are completely remineralized. The size distribution for single particle at depth z' is $N(d, z') = C_{p,d} m_d \sim (1 - \psi z')^{-1}$. At $z' \to h_0$ $N(d, z') \to \infty$ while $m_d \to 0$. The finite thickness of the layer of sinking particles with parameters given in Table 1 varies in the range from 41.3 m at $d_0 = 20$ μm to 9937 m at $d_0 = 20$ μm. Note that the solution to the problem in a different formulation (Omand et al., 2020) has qualitatively the same character. However, the profiles of total POM concentration and total POM flux decay asymptotically approaching to the exponential, in contrast to the profiles

https://doi.org/10.5194/egusphere-2025-491
Preprint. Discussion started: 21 February 2025

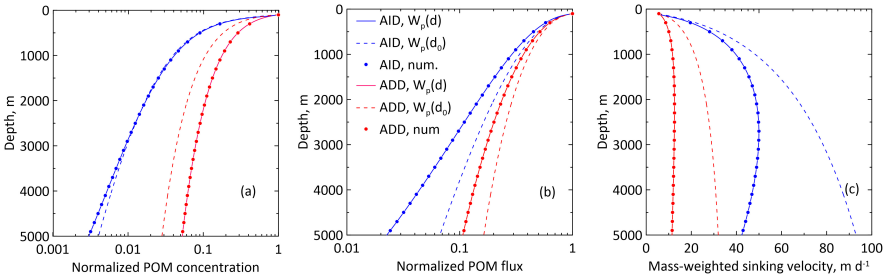

Figure 1. The normalized POM concentration C_p (a), total POM flux F_p (b), and weighted vertical velocity of particles (c) for AID and ADD models calculated from analytical and numerical solutions. The dashed line corresponds to the solution of 1 at constant $W_p(d_0)$, while the solid line corresponds to the solution of the problem at variable $W_{p,d}$)

(17) and (18) for one class of particle sizes on $z' = 0$. These profiles normalized to values at the base of the euphotic layer are shown in Fig. 1 where C_p and F_p profiles were obtained by summation of n_d profiles in (16) and (18). The baseline parameters for calculation are given in Table 1. These parameter values match those used by DeVries et al. (2014). Therefore, the curves in Fig. 1 also coincide with the corresponding curves in Fig. 1c from (DeVries et al., 2014) calculated using another but equivalent formulation of the same problem as shown in Appendix.

In contrast to the AID model solution (16), the POM concentration profile (28) decays asymptotically with depth at $\zeta > \eta$ and $\zeta > \eta\beta$ for the ADD model (20). These conditions are met for the parameters listed in Table 1. The rate of degradation γ also decays with depth; the corresponding exponent in (25) differs from the parameter β in the models with a constant sinking rate (32). A sensitivity to the AID model parameters was considered by DeVries et al. (2014). They found that of the four parameters controlling the flux profile (η, ζ, γ_0, ϵ), the most significant is the slope of the particle distribution ϵ on $z' = 0$, which has the greatest influence on the depth distribution of particles. As follows from Fig. 2 in which the variables are presented in logarithmic coordinates, only the vertical distribution of C_p is close to the power distribution with an exponent of about 1, while the distribution with the depth of the total particle flow F_p significantly deviates from the power law dependence (Martin's law). The sensitivity of concentration and flux profiles to the values of α and β parameters is examined in Figure 2. An increase in the parameter α leads to a deepening of the concentration and particle flux profiles, while an increase in the β leads to shallowing of these profiles.

4 Numerical model

4.1 Numerical algorithm

The model discussed in the previous section is based on several simplifying assumptions that made it possible to obtain analytical solutions to the system of equations. However, when we expand the model to include new important factors in the

https://doi.org/10.5194/egusphere-2025-491
Preprint. Discussion started: 21 February 2025

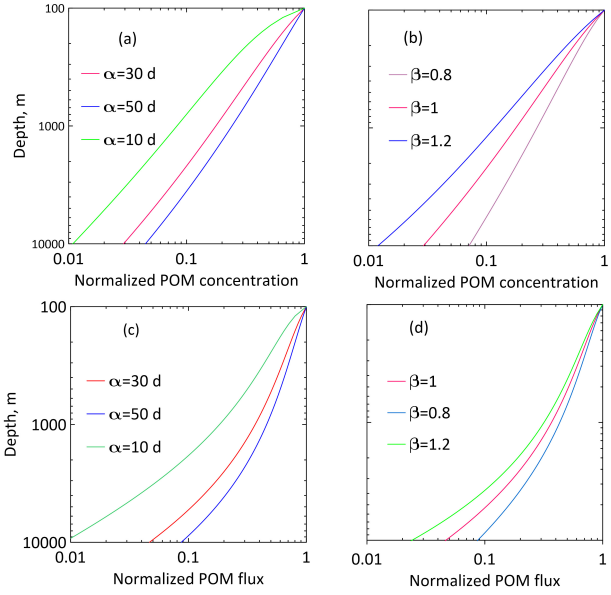

Figure 2. The normalized total particle concentration C_p (a) and total particle flux F_p (b) sensitivity to parameters α and β.

processes of sinking and remineralization of POM, analytical solutions to the problem can no longer be obtained. Therefore, a numerical Eulerian-Lagrangian approach to solving the problem was developed.

Here we will limit ourselves to the case where the degradation rate depends on the age of the organic particle (ADD model), the temperature of sea water T and the concentration of oxygen $[O_2]$:

$$\gamma = \gamma(t, T(z'), [O_2](z')) = \left(\frac{\beta}{\alpha + t}\right)\left(Q_{10}^{\frac{T-T_{ref}}{10}}\right)\left(\frac{[O_2]}{K_O + [O_2]}\right), \tag{33}$$

where Q_{10} is the temperature coefficient, T_{ref} is a reference temperature, K_{O2} (kg m^{-3} is an oxygen dependence parameter (Cram et al., 2018). When γ does not depend on age (AID model) then

$$\gamma = \gamma_0 \left(Q_{10}^{\frac{T-T_{ref}}{10}}\right)\left(\frac{[O_2]}{K_O + [O_2]}\right), \tag{34}$$

The system of Lagrangian equations for particle depth and size derived from (3) - (5) is

$$\frac{\partial d}{\partial t} = -\frac{\gamma(t, T(z'), [O_2](z')}{\zeta} d, \tag{35}$$

$$\frac{\partial z'}{\partial t} = c_w d^{\eta}. \tag{36}$$

The initial conditions are that at $t = 0 : z' = 0 \,\text{and}\, d = d_{0,i}$.

The procedure of finding the profiles of $C_p(z')$ and $F_p(z')$ is as presented in Fig. 3. It includes 11 steps.

Step 1 The model parameters and temperature and oxygen concentration profiles are read from the input files.

https://doi.org/10.5194/egusphere-2025-491
Preprint. Discussion started: 21 February 2025

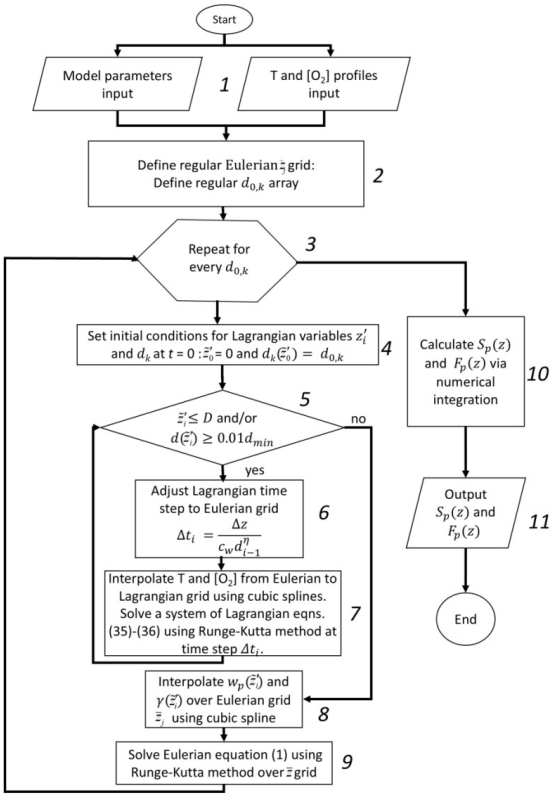

Figure 3. The Eulerian-Lagrangian method flow chart for equations of sinking particulate organic matter.

Step 2 The regular Eulerian grid $\bar{z}'$ is set up from 0 to the ocean depth D on n_z equal intervals Δz with levels $\bar{z}' = j \cdot \Delta z$, where $j = (0, n_z)$. The particle size spectrum at the lower boundary of the euphotic layer is divided on n_d equal intervals of size Δd in the range from d_{min} to d_{max}. For every particles size $d_{0,k}$, $k = (0, n_d)$.

Step 3 Sequential steps 4-9 are performed for every $d_{0,k}$, $k = (0, n_d)$. Then move to the Step 10.

Step 4 Set the initial conditions for Lagrangian particle depth $\tilde{z_k}'(t_i)$ and size $d = d_{0,k}$ equations at $t_i = 0$.

Step 5 If Lagrangian particle depth $\tilde{z_k}'(t_i)$ is equal or greater than ocean depth D and/or particle diameter on this depth level $d = d_{0,k}$ is equal or less than 1% of minimum diameter size d_{min} then perform Step 8 else perform Step 6.

Step 6 The timescale is divided on the intervals Δt_i, $i = (0, n_t)$ over which equations (35)-(36) are integrated. To align the resulting $\tilde{z_k}'(t_i)$ and regular depth grid $\bar{z}'$, the i-th timestep duration is calculated as $\Delta t_{i,k} = \Delta z / (c_w d_{i,k}^{\eta})$.

Step 7 Using the Lagrangian formulation with respect to time t solve a system of equations (35)-(36) using Runge-Kutta's method of the 4th order. The cubic spline interpolation is used to calculate the temperature and oxygen concentration at $\tilde{z_k}'(t_i)$.

https://doi.org/10.5194/egusphere-2025-491
Preprint. Discussion started: 21 February 2025

Step 8 The $w_p(\tilde{z_k}'(t_{i+1}))$ and $\gamma(\tilde{z_k}'(t_{i+1}))$ profiles at the Lagrangian grid of are interpolated using cubic spline over the Eulerian grid $\bar{z}'$.

Step 9 The $C_(p,d)(\bar{z}')$ is calculated by solving Eulerian equation (1) with Runge-Kutta method over the regular grid $\bar{z}'$. Then move to Step 3.

Step 10 The total POM concentration $C_p(\bar{z}')$ and POM flux $F_p(\bar{z}')$ are obtained via numerical integration of $S_(p,d)(\bar{z}')$ and $w_p(\bar{z}'))$ by using the composite Simpson's 1/3 rule.

Step 11 Model output: total POM concentration $C_p(\bar{z}')$ and POM flux $F_p(\bar{z}')$.

The code for the proposed algorithm along with the data used in this study, is archived on Zenodo (Kovalets et al., 2025a, b).

4.2 Numerical model setup

The simulations were carried out for the water column of depth $D = 5000$m, $n_z = 1000$, and $\Delta z = 1$m. We calculate the vertical profiles of POM concentration C_p and flux F_p using AID and ADD models for degradation rate. The rest of the model parameters, except η, were adopted from Table 1. In Fig.1 the profiles of C_p and F_p were calculated using an above algorithm and $\eta = 1.17$ to be compared with analytical solutions for AID and ADD parameters from Table 1. As seen in the figure numerical and analytical profiles coincide.

The calculations were compared with the available measurement data for C_p and F_p for the latitude band of 20-30°N in the Atlantic and Pacific Oceans and 50-60°S of the Southern Ocean. These calculations aimed to assess the relative influence of the vertical distribution of temperature and oxygen in Atlantic, Pacific and Southern oceans on profiles C_p and F_p. For the Atlantic Ocean, C_p and F_p data are compiled in (Aumont et al., 2017) and (Lutz et al., 2002) while for the Pacific Ocean, they are given in (Martin et al., 1987) and (Druffel et al., 1992). The Southern Ocean data for Pacific and Atlantic sectors are given in (Aumont et al., 2017) and (Lutz et al., 2002). The required for calculations averaged over the region and time profiles of T and $[O_2]$ were constructed using the measurement data from (Boyer et al., 2018). These averaged profiles are shown in Fig. S1 in the Supplement. It is necessary to emphasize the great uncertainty not only in the choice of model parameter values but also in the processes' parameterization. This is explained by both an insufficient understanding of the physical and biogeochemical processes, and the lack of a sufficient number of measurements in the deep layers of the ocean. In particular, the observation results (Cael et al., 2021) show large deviations in the parameters of the sinking velocity-particle size relationship (3). In the recent models parameter η varies in range from 0.26 (Alcolombri et al., 2021) to 2 (Omand et al., 2020). Therefore in simulations we compare effect of η on C_p and F_p profiles for two values: $\eta = 1.17$ (Smayda, 1970) and $\eta = 0.63$ (Cael et al., 2021).

5 Modelling results

Figures 4-6 show the profiles C_p and F_p normalised to $C_p(z_{eu})$ and $F_p(z_{eu})$. They were calculated using the numerical algorithm described in Section 4.1. These profiles are compared with normalised measurements in the subtropical zones of the Atlantic and Pacific oceans, and also in the Atlantic and Pacific sectors of Southern Ocean to consider temperature and oxygen

https://doi.org/10.5194/egusphere-2025-491
Preprint. Discussion started: 21 February 2025

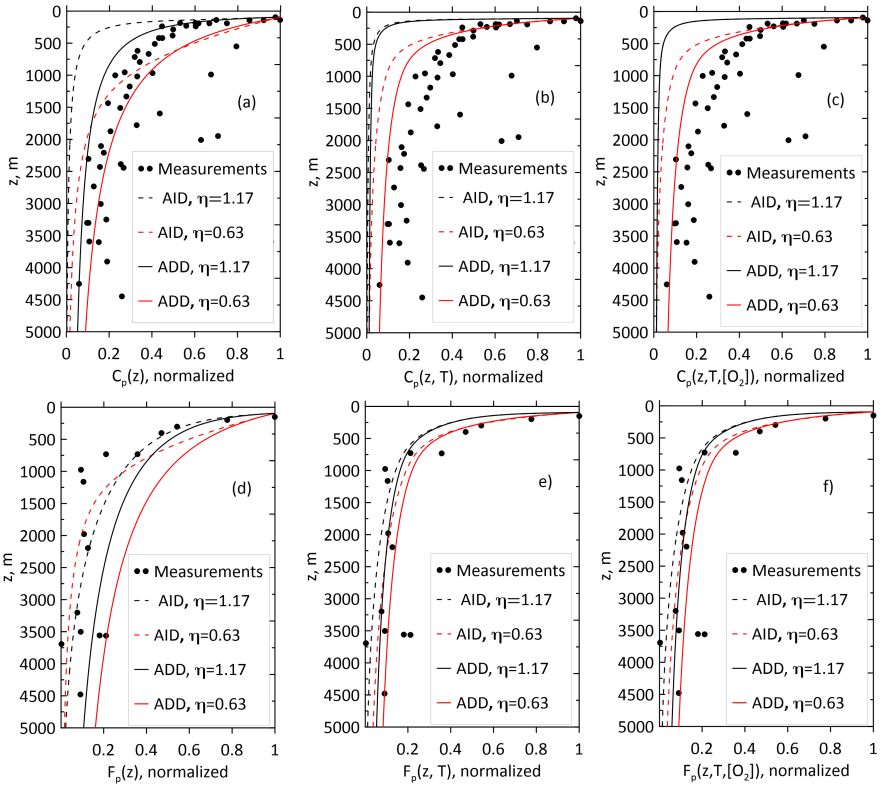

Figure 4. The normalized total POM concentration C_p (a-c) and total POM flux F_p (d-f) versus measurement data in the Atlantic Ocean at 20-30°N (Aumont et al., 2017; Lutz et al., 2002).

concentration effects on POM. The C_p and F_p profiles in Figures 4-6 were obtained for three variants of the degradation model. In the first variant (plots a and d), C_p and F_p do not depend on temperature and oxygen concentration. in the second variant (plots b, e) they do not depend on oxygen concentration, and in the third variant (c, f) they depend on temperature, and oxygen concentration. The first variant is described by analytical solutions for AID and ADD models. The features of these solutions
255 are discussed in Section 3.3. The profiles of C_p and F_p are sensitive to the value of η. The solutions with $\eta = 0.63$ decay slower than obtained for $\eta = 1.17$ as follows also from analytic solutions.

Using the AID model leads to a more rapid decay of C_p with depth than was observed in all ocean profiles. At the same time, the decay of F_p with depth occurs more slowly in most of the measured profiles. The using of ADD model (Figs. 4-6) results in more smooth profiles, however qualitatively AID and ADD profiles are close.

260 As can be seen from Fig. 4-6, the dependence of the degradation rate on temperature significantly affected the profiles of C_p and F_p enhancing the degradation of sinking particles in the upper layers of the ocean and suppressing it in the deep layers of the ocean. The influence of oxygen concentration in all cases considered was less significant compared to the distribution of temperature with depth. Overall, including temperature and concentration dependence in the degradation rate relationship

https://doi.org/10.5194/egusphere-2025-491
Preprint. Discussion started: 21 February 2025

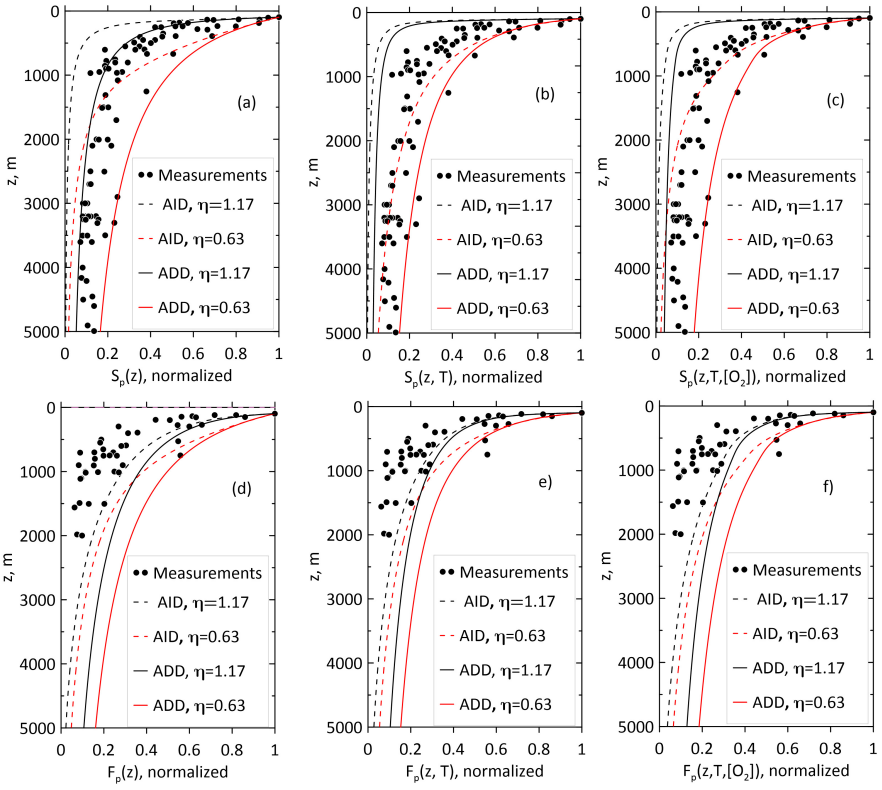

Figure 5. The normalized total POM concentration C_p (a-c) and total POM flux F_p (d-f) versus measurement data in the Pacific Ocean at 20-30°N (Martin et al., 1987; Druffel et al., 1992)

improves the agreement with ocean measurements. The normalized Mean Bias Errors (MBE) when taking into account the dependence of the degradation rate on temperature and oxygen concentration (third variant) are reduced from 9% to -3% compared to first variant when this dependence was not taken into account. For third variant the Root Mean Square Deviation (RMSD) decreased by half comparatively with first variant. Notice that both AID and ADD models somewhat underestimates F_p when dependence on temperature is taken into account. As follows from Figs. 4-6, the use of a AID model leads to a more rapid decay of S_p and with depth than was observed in all ocean profiles. At the same time, the decay of F_p with depth occurs more slowly in most of the measured profiles. The using of ADD model (Figs. 4-6) results in more smooth profiles, however qualitatively AID and ADD profiles are close.

As follow from Fig. 4-6 the model output was sensitive to the parameters with high uncertainty such as η. Therefore, a sensitivity study was carried out for the model parameters in Table S1. We used the one-at-a-time method to quantify the effect of the variation of a given parameter on the model output while all other parameters were kept at their initial values (Hamby, 1994; Lenhart et al., 2002; Soares, 2021). The effects of variations in these parameters were estimated for the particle transfer efficiency (TE). Define TE_{1000} as the ratio of the concentration of POM at the lower level of the euphotic layer z_{eu} to the

https://doi.org/10.5194/egusphere-2025-491
Preprint. Discussion started: 21 February 2025

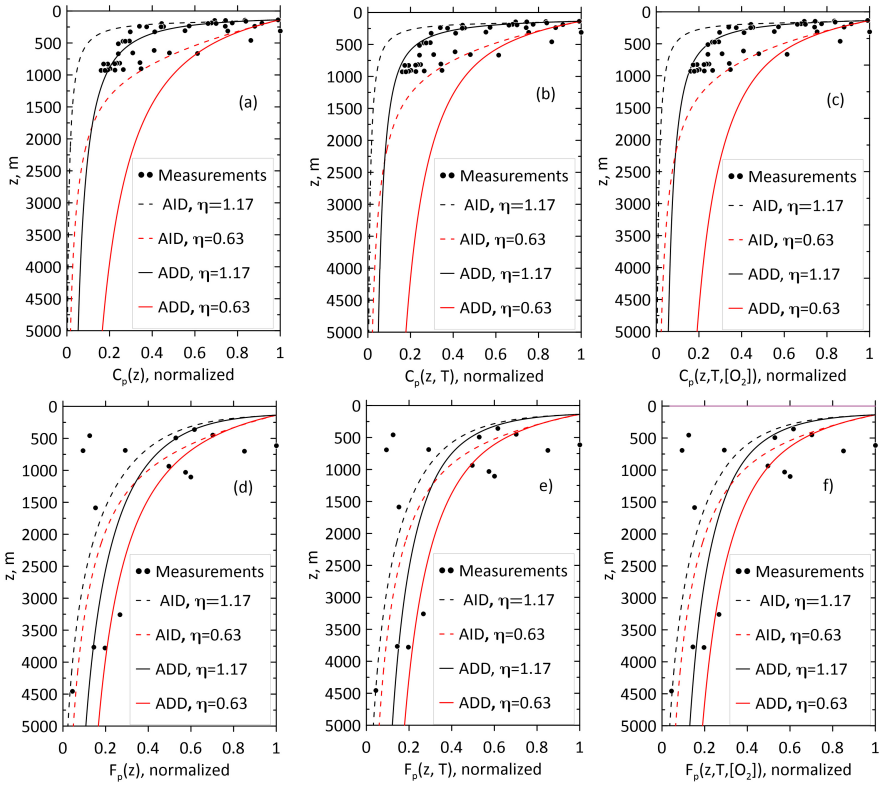

Figure 6. The normalized total POM concentration C_p (a-c) and total POM flux F_p (d-f) versus measurement data in the Southern Ocean at 50-60°N (Aumont et al., 2017; Lutz et al., 2002)

concentration at the lower boundary of the mesopelagic layer $z = 1000$ and TE_{5000} as the ratio of the concentration of POM at the lower level of the euphotic layer to the concentration in the bottom layer at $z = 5000$m.

The range for parameters is defined as follows: minimum parameter value p_{min} was set to be proportional to the reference value p_{ref} with a ratio value $1/r < 1$ and maximum value p_{max} was set to be proportional to p_{ref} with a ratio value $r > 1$ to the reference value. For all parameters in Table S1, the value of r was chosen the same ($r = 1.25$). This value satisfies to ranges of all parameters. The model output sensitivity was estimated using a sensitivity index (SI) defined as

$$SI = \frac{TE(p_{max}) - TE(p_{min})}{TE(p_{ref})}, \tag{37}$$

where $TE(p_{max})$, $TE(p_{min})$ and $TE(p_{ref})$ are the simulation results for maximal p_{max}, minimal p_{min}, and reference p_{ref} parameter values, respectively. Calculations of SI were carried out for the Pacific Ocean for AID and DDR models using reference, maximal and minimal values of parameters from Table S1.

The sensitivity index TE_{1000} is shown in Fig. S2 in the Supplement for the parameters of AID model. As seen in the figure, $TE_{1000}$is most sensitive to the exponent ζ in the power law dependence of particle mass on particle size (4) and to the

https://doi.org/10.5194/egusphere-2025-491
Preprint. Discussion started: 21 February 2025

exponent ϵ in the power law dependence of particle size distribution at the lower boundary of the euphotic layer (13). The sign of the index shows if the model reacts codirectionally to the input parameter change, i.e., if the parameter increase /decrease corresponds to the increase/decrease of the model output parameter. The nature of the dependence of TE_{1000} on ζ and ϵ is different. The increase ζ results in an increase TE_{1000}, i.e. increase in the mass of a particle increases transfer efficiency. At the same time, the increase ϵ results in a decrease TE_{1000}, i.e. an increase in the slope of the spectral particle size distribution leads to a decrease of transfer efficiency. The dependence of TE_{1000} on T_{ref} and K_O was weak ($SI << 1$), whereas dependence on γ_0, η and Q_{10} was moderate. The sensitivity index $SI(TE_{5000})$ for parameters of the AID model is shown in Fig. S3. As seen in the figure, it is qualitatively similar to Fig. S2. Four parameters ($\gamma_0, \zeta, \eta, \epsilon$) show strong sensitivity.

The sensitivity index TE_{1000} for parameters of the ADD model is shown in Fig. S4. Similarly, Fig. S2. TE_{1000} is most sensitive to ζ and ϵ, however, amplitudes of TE_{1000} are less than for AID model. The dependence on ADD model parameters (α and β) are moderate. The sensitivity index TE_{5000} for parameters of the ADD model is shown in Fig. S5. It similar to the TE_{1000} for this model, but the amplitudes of TE_{5000} are greater than TE_{1000} amplitudes. More details of the sensitivity study are given in the Supplement.

6 Conclusions

In this paper, we considered simple Eulerian-Lagrangian approach to solve equations describing gravitational sinking of organic particle under influence of the size and age of particles, temperature and oxygen concentration on their dynamics and degradation processes. The novel analytical solutions of the system of the one-dimensional Eulerian equation for POM concentration and Lagrangian equations for particle mass and depth were obtained for constant and age-dependent degradation rates. It was found that feedback between degradation rate and sinking velocity results to a significant change in POM and POM flux profiles. In the case of constant γ_0 (AID model), the vertical distribution of concentration $C_{p,d}$ for single fraction of POM size d_0 at z_{eu} is limited by a finite layer. Particles in this layer sink at a linearly decreasing velocity. At the same time, the distribution of total particle concentration C_p and flux F_p approaches exponential with depth for increase of d_0 fractions. In contrast to AID model, the vertical distribution of concentration and vertical velocity decay asymptotically with depth for ADD model. The rate of degradation in Eulerian variables decays with depth, however the corresponding exponent depends not only on the parameter β as the models with a constant sinking velocity (Cael et al., 2021), but also on the parameters characterizing the vertical velocity of particles η and their porosity ζ. With baseline parameters the vertical distribution of C_p is close to the power distribution with an exponent of about 1, while the distribution with the depth of the total particle flow F_p significantly deviates from the power law dependence ("Martin's law").

A new Eulerian-Lagrangian numerical approach to solving the problem in general cases was presented. It allows to include in consideration of different parameterizations of interacted degradation and sinking processes. However, here we limited ourselves to the case where the degradation rate depends on the age of the organic particle, the temperature of sea water and the concentration of oxygen. The numerical method was tested on the obtained analytical solutions

https://doi.org/10.5194/egusphere-2025-491
Preprint. Discussion started: 21 February 2025

The calculations are compared with the available measurement data for POM and POM flux for the latitude band of 20-30°N in the Atlantic and Pacific Oceans and 50-60°S in the Southern Ocean. The dependence of the degradation rate on temperature significantly affected the profiles of total particle concentration and flux enhancing the degradation of sinking particles in the upper layers of the ocean and suppressing it in the deep layers of the ocean. Overall, including temperature and concentration dependence in the degradation rate relationship improves the agreement with ocean measurements. In particular, normalized MBEs when taking into account the dependence of the degradation rate on temperature and oxygen concentration are reduced from 9% to -3% compared to cases when this dependence was not taken into account. Similarly, on the average, RMSD decreased by half when taking into account temperature stratification.

Discrepancies between model predictions and observations are caused by incomplete description of processes and uncertainty of model parameters, as well as variability of measured POM concentration profiles due to vertical and horizontal variability of ocean fields. We used the one-at-a-time method to quantify the effect of the variation of one the parameter from set $(\gamma_0, \eta, \zeta, \epsilon, T_{ref}, Q_{10}, K_0, \alpha, \beta)$ on the model output while all other parameters were kept at their initial values. The effects of variations in these parameters were estimated for the particle transfer efficiency TE as ratio of POM flux on z_{eu} to value on the depth of 1000 m or 5000 m. The model output sensitivity was estimated using a sensitivity index SI (37). Calculations for the Pacific Ocean showed that TE_{1000} and TE_{5000} are most sensitive to the parameters ζ and ϵ for both models. Therefore, calibration and optimization of these parameters should be primarily carried out.

It should be noted that to obtain analytical solutions and demonstrate the numerical Euler-Lagrangian approach, significant simplifications were made in the description of particle dynamics. In particular, the particle sinking velocity was described in the Stokes approximation, aggregation and fragmentation of particles, mineral ballasting, ocean density stratification, and temporal changes in particle flows were not taken into account. While some simplifications can be eliminated by using a numerical approach, others require significant generalization.This particularly applies to the description of particle ballasting mechanisms. On the one hand, ballast affects the sinking of particles, but on the other hand, ballast minerals can protect organic matter from remineralization (Cram et al. 2018). In addition, the mechanisms regulating the distribution of particles of different nature between aggregates and free particles are also unclear. These circumstances did not allow the inclusion of ballasting parameterizations in the present model.

Code and data availability. The exact version of the model used to produce the results used in this paper is archived on Zenodo (Kovalets et al., 2025a), as are input data to run the model and produce the plots for all the simulations presented in this paper (Kovalets et al., 2025b).

Appendix A: Derivation of the spectral solution for size distribution (DeVries et al., 2014)

Here we will show that analytical solution (14) for $C_{p,d}$ is equivalent to the solution (8) from (DeVries et al., 2014) of the spectral equation for particle size distribution. To find particle size distribution at z' we first re-arrange equation (12) obtaining

https://doi.org/10.5194/egusphere-2025-491
Preprint. Discussion started: 21 February 2025

the relation between d_0 and d at depth z':

$$d_0 = d(1+\psi z')^{1/\eta}. \tag{A1}$$

The size distribution $N(d,z)$ [m^{-4}] is related with $C_{p,d}$ and m_d as

$$C_{p,d} = N m_d \Delta d. \tag{A2}$$

where Δd is a small size increment. Combining (14), (3), (12), and (A2) gives

$$N(d,z') = \frac{C_{p,d}}{m_d \Delta d} = \frac{\Delta d_0}{\Delta d} M_0 d_0^{-\epsilon} \left(1 + \frac{\eta\gamma_0}{\zeta c_w d^\eta} z'\right)^{\frac{\eta-\epsilon}{\eta}}. \tag{A3}$$

In the limit of $\Delta d \to 0$ we obtained

$$\lim_{\Delta d \to 0} \frac{\Delta d_0}{\Delta d} = \frac{d}{dd} d_0 = \left(1 + \frac{\eta\gamma_0}{\zeta c_w d^\eta} z'\right)^{\frac{1-\eta}{\eta}}. \tag{A4}$$

Then Eqn.(A3) can be written as

$$N(d,z') = M_0 d^{-\epsilon} \left(1 + \frac{\eta\gamma_0}{\zeta c_w d^\eta} z'\right)^{\frac{1-\epsilon}{\eta}}. \tag{A5}$$

This solution for N coincides with that found by DeVries et al. (2014).

Author contributions. VM-Conceptualization, VM, IB - Methodology, KK, KOK - Software, SS - Visualization, KOK, KK, SS- Investigation. VM, IB, and KK - Writing - original draft, KOK and SS- Writing - review and editing, VM - supervision. All authors contributed to the interpretation of the findings and the writing of the paper.

Competing interests. The contact author has declared that none of the authors has any competing interests.

Acknowledgements. The research is supported by the National Research Foundation of Ukraine project no. 2023.03/0021, and the Korea Institute of Marine Science and Technology Promotion (KIMST) funded by the Ministry of Oceans and Fisheries (RS-2023-00256141).

https://doi.org/10.5194/egusphere-2025-491
Preprint. Discussion started: 21 February 2025

References

Alcolombri, U., Peaudecerf, F.J., Fernandez, V.I. Lars Behrendt, L., Lee K. S., and Stocker, R.: Sinking enhances the degradation of organic particles by marine bacteria, Nat. Geosci. 14, 775–780. https://doi.org/10.1038/s41561-021-00817-x, 2021.

Armstrong, R.A., Lee, C., Hedges, J.I., Honjo, S., and Wakeham, S.G.: A new, mechanistic model for organic carbon fluxes in the ocean based on the quantitative association of POC with ballast minerals, Deep-Sea Res. II, 49, 219–236, 2002.

Aumont, O., van Hulten, M., Roy-Barman, M., Dutay, J.-C., Éthé, C., and Gehlen, M.: Variable reactivity of particulate organic matter in a global ocean biogeochemical model, Biogeosciences, 14, 2321–2341, https://doi.org/10.5194/bg-14-2321-2017, 2017.

Banse, K.: New views on the degradation and disposition of organic particles as collected by sediment traps in the open ocean, Deep Sea Res. A 37, 1177–1195, https://doi.org/10.1016/0198-0149(90)90058-4, 1990.

Boyer, T.P., Baranova,O.K., Coleman, C. , Garcia, H.E., Grodsky, A., Locarnini, R.A., Mishonov, A.V. , Paver, C.R., Reagan, J.R., Seidov, D., Smolyar, I.V., Weathers, K., and Zweng,M.M.: World Ocean Database 2018. A.V. Mishonov, Technical Ed., NOAA Atlas NESDIS 87. https://www.ncei.noaa.gov/sites/default/files/2020-04/wod_intro_0.pdf, 2018.

Burd, A. B.: Modeling the vertical flux of organic carbon in the global ocean, Annu. Rev. Mar. Sci. 16:135–61, 2024.

Cael, B. B., Cavan, E. L., and Britten,G. L.: Reconciling the size dependence of marine particle sinking speed, Geophysical Research Letters, 48, e2020GL091771. https://doi.org/10.1029/2020GL091771, 2021.

Cram, J. A., Weber, T., Leung, S. W., McDonnell, A. M. P., Liang, J.-H., and Deutsch, C.: The role of particle size, ballast, temperature, and oxygen in the sinking flux to the deep sea, Global Biogeochemical Cycles, 32, 858–876. https://doi.org/10.1029/2017GB005710, 2018.

DeVries, T., Liang, J.H., and Deutsch, C.: A mechanistic particle flux model applied to the oceanic phosphorus cycle. Biogeosciences, 11, 5381–98, 2014.

Druffel, E., Williams, P., Bauer, J., and Ertel, J.: Cycling of dissolved and particulate organic matter in the open ocean, J. Geophys. Res., 97, 15639–15659, https://doi.org/10.1029/92JC01511, 1992.

Hamby, D.M.: A review of techniques for parameter sensitivity analysis of environmental models, Environ. Monit. Assess. 32, 135–154.

Jokulsdottir, T. and Archer, D.: A stochastic, Lagrangian model of sinking biogenic aggregates in the ocean (SLAMS 1.0): model formulation, validation and sensitivity, Geosci. Model Dev., 9, 1455–1476, https://doi.org/10.5194/gmd-9-1455-2016, 2016.

Kostadinov, T. S., Siegel, D. A., and Maritorena, S.: Retrieval of the particle size distribution from satellite ocean color observations, J. Geophys. Res., 114, C09015, https://doi.org/10.1029/2009JC005303, 2009.

Kovalets, K., Maderich, V., Brovchenko, I., Seo, S., and Kim, K. O.: KKovalets/EuLag: EuLag (v0.2.0). Zenodo. https://doi.org/10.5281/zenodo.14782046, 2025a.

Kovalets, K., Maderich, V., Brovchenko, I., Seo, S., and Kim, K. O.: KKovalets/EuLag_DataSet: EuLag_DataSet (v0.0.0). Zenodo. https://doi.org/10.5281/zenodo.14782095, 2025b.

Kriest, I. and Oschlies, A.: On the treatment of particulate organic matter sinking in large-scale models of marine biogeochemical cycles, Biogeosciences, 5, 55–72, https://doi.org/10.5194/bg-5-55-2008, 2008.

Lenhart, T., Eckhardt, K., Fohrer, N., Frede, H.G.: Comparison of two different approaches of sensitivity analysis, Phys. Chem. Earth, 27, 645–654. https://doi.org/10.1016/S1474-7065(02)00049-9, 2002.

Lutz, M. J., Dunbar, R. B., and Caldeira, K.: Regional variability in the vertical flux of particulate organic carbon in the ocean interior, Global Biogeochem. Cycles, 16, 1037, https://doi.org/10.1029/2000GB001383, 2002.

https://doi.org/10.5194/egusphere-2025-491
Preprint. Discussion started: 21 February 2025

Maderich, V., Kim, K.O., Brovchenko, I, Jung, K.T., Kivva, S., and Kovalets, K.: Dispersion of particle-reactive elements caused by the phase transitions in scavenging, Journal of Geophysical Research, 127, e2022JC019108.https://doi.org/10.1029/2022JC019108, 2022.

Martin, J., Knauer, G., K., D., and Broenkow, W.: VERTEX: carbon cycling in the northeast Pacific, Deep-Sea Res., 34, 267–285, 1987.

McDonnell, A. M., and Buesseler, K. O. Variability in the average sinking velocity of marine particles, Limnology & Oceanography,55(5), 2085–2096. https://doi.org/10.4319/lo.2010.55.5.2085, 2010.

Middelburg, J.: A simple rate model for organic matter decomposition in marine sediments, Geochim. Cosmochim. Ac., 53, 1577–1581, doi:10.1016/0016-7037(89)90239-1, 1989

Mullin, M., Sloan, P. R., and Eppley, R. W.: Relationship between carbon content, cell volume, and area in phytoplankton, Limnol. Oceanogr., 11, 307–311, 1966.

Omand, M. M., Govindarajan, R., He, J., and Mahadevan, A. Sinking flux of particulate organic matter in the oceans: sensitivity to particle characteristics, Sci. Rep. 10, 5582. https://doi.org/10.1038/s41598-020-60424-5, 2020.

Roca-Martí, M., and Puigcorbé, V.: Combined use of short-lived radionuclides (^{234}Th and ^{210}Po) as tracers of sinking particles in the ocean, Annu. Rev. Mar. Sci. 16, 551–575. https://doi.org/10.1146/annurev-marine-041923-013807 2024.

Sheldon, R.W., Prakash, A., and Sutcliffe Jr.,W.: The size distribution of particles in the ocean, Limnol. Oceanogr., 17, 327–339,1972.

Siegel, D. A., DeVries, T., Cetini, I., and Bisson, K. M.: Quantifying the ocean's biological pump and its carbon cycle impacts on global scales, Annu. Rev. Mar. Sci. 15, 329–356. https://doi.org/10.1146/annurev-marine-040722-115226, 2023.

Smayda, T. The suspension and sinking of phytoplankton in the sea, Oceanogr. Mar. Biol., 8, 353-414, 1970.

Soares, L.M.V, Calijuri, M.C. Sensitivity and identifiability analyses of parameters for water quality modeling of subtropical reservoirs, Ecol. Modell. 458, 109720, 2021.